Osmotic pressure induced toxicity by aggregation of citrate-coated silver nanoparticles inside HepG2 cells

Pamela C. Ubaldo,[1] Henok D. Abshiro,[1] Franklin A. Cavender,[1] Jay C. Means,[2,*] Dale Buchanan Hales,[3,*] and Lichang Wang[1,*]

[1]Department of Chemistry and Biochemistry, Southern Illinois University, Carbondale, IL 62901, United States;
[2]Bren School for Environmental Science & Management and Earth Research Institute, University of California-Santa Barbara, Santa Barbara, CA 93106, United States;
[3]Department of Physiology, School of Medicine, Southern Illinois University, Carbondale, IL 62901, United States

Abstract

The effects of 10nm citrate-coated silver nanoparticles (AgNPs) to hepatocellular carcinoma (HepG2) cells were investigated to elucidate toxicity mechanisms. Cell viability, oxidative stress, protein expression, and cell morphology were assessed to determine the toxicity of AgNPs at various dose levels. 10nm citrate-coated AgNPs were found to be toxic to HepG2 cells at a dose of > 1.0 ppm and their LD_{50} was determined to be 3.0 ppm. Oxidative stress levels in the cells were found to increase with the dose of AgNPs and HepG2 cells can withstand high level of reactive oxygen species before cell death. The expressions of heat shock proteins and tubulin proteins were most significantly affected by the presence of AgNPs of 5.0 ppm. The AgNPs were observed to penetrate the cells treated with a dose of 5.0 ppm by transmission electron microscopy. Furthermore, the agglomeration of AgNPs in HepG2 cells was found and generated osmotic pressure that is likely another pathway to be responsible for the toxicity of AgNPs.

* Corresponding authors: lwang@chem.siu.edu (LW); toxdoc796@gmail.com (JCM); dhales@siumed.edu (DBH)

1. Introduction

Silver nanoparticle (AgNP) is one of the emerging and fastest growing materials in the field of nanotechnology [1-3] and Biomedicine[4-8] that benefited from the advancements in the studies of nanoparticles[9-14] and applications such as in catalysis[15-28]. The rapid growth of Ag-based nanomaterials is attributed to silver's antimicrobial properties [29-35], good optical, conductive, and other outstanding properties [36-39]. AgNPs have becoming a part of common daily exposures in humans because of its use in topical wound dressings, clothing, cosmetics, water filters, laundry detergent, electronics, and many other applications [36-39].

In 2008, the International Center for Technology Assessment (CTA) and a coalition of consumer, health, and environmental groups filed a legal action for the Environmental Protection Agency (EPA) to stop the sale of over two hundred (200) nanosilver products [40]. This event resulted in more curiosity and controversy about the toxicity of AgNPs. Several toxicity studies have since become available by examining the effects of various factors such as nanoparticle size, stabilizer, dosage, cell type, and biochemical assay [2, 36, 41-57]. Studies have shown that toxicity of AgNPs is dependent on the size, shape, and stabilizer [39, 58-60]. El Badawy, et. al. attributed the toxicity to the surface charge of AgNPs that is dependent on the stabilizer used (positive is more toxic) [36]. Lankoff, et. al. suggested that size and agglomeration of AgNP can contribute to biological impact [42]. Other studies attributed the toxicity to the Ag cations that possibly leak out of AgNPs [45, 61-65]. In spite of the rapid growth and increasing use of a variety of AgNPs, toxicity assessments of AgNPs remain to be further investigated.

The exposure of AgNPs can be through inhalation, ingestion, or topical application [38]. The study by Garza-Ocanas, et. al. has shown that, upon long term exposure to AgNPs, the most affected organ is the liver [45]. As such, we chose to study the toxicity of AgNPs to HepG2 cells.

47 Our work aims to understand the toxicity of 10nm citrate-coated AgNPs to HepG2 cells,
48 particularly the toxicity mechanism and how these AgNPs affect cell viability, cell morphology,
49 oxidative stress, and protein expression. Furthermore, this study intends to locate AgNPs in or
50 outside the cell and to determine the effect of AgNPs to the protein expression when the cells are
51 exposed to a high dose of these citrate-coated AgNPs.

52 **2. Materials and methods**

53 *2.1 Materials*

54 Citrate-coated silver nanoparticles (AgNPs) with a diameter of 10nm were purchased from
55 Nanocomposix (United States). Hepatocellular carcinoma (HepG2) cells were purchased from
56 ATCC (United States). All other reagents were reagent grade and were purchased from Fisher
57 Scientific (Saint Louis, Mo, USA) or were used as supplied from assay kit manufacturers.

58 *2.2 Cell culture*

59 The HepG2 cells were cultured in complete growth media containing 10% fetal bovine
60 serum, 1% non-essential amino acids, 1% of 100mM sodium pyruvate, 1% Penicillin-
61 Streptomycin 10/10 (Atlanta Biologicals, Atlanta, GA, USA), 2.5% of 1M HEPES buffer
62 solution, and 84.5% minimum essential media. Cells were grown to approximately 85%
63 confluence and subcultured to a ratio of 1:4 every three days. Cells were incubated at 37ºC in a
64 5% CO_2 humidified incubator. Proliferation of HepG2 cell lines was performed in the presence
65 of AgNPs (0-10.0 ppm) and cell viability was assessed as described below.

66 *2.3 Cell viability test*

67 Approximately $4x10^4$ cells were seeded onto a 48-well plate and grown to approximately
68 60% confluence. Then different doses of citrate stabilized, i.e. citrate-coated, AgNPs for 24h

69 were applied to the wells. The doses of citrate stabilized AgNPs were 0.3, 0.5, 0.75, 1.0, 1.5, 3.0,
70 and 5.0 ppm.

71 Stabilizer control HepGe cells dosed with 0.1 μM citrate for 24 hours and no treatment
72 control HepG2 cells were also prepared. The cytotoxic effect with the increasing dose of citrate
73 stabilized AgNPs was then assessed.

74 After 24 hours of treatment, HepG2 cells were washed with MEM (minimum essential
75 medium), trypsinized, and incubated at 37°C in 5% CO_2 humidified incubator and resuspended
76 in complete growing media. The cells were then dyed with tryphan blue and counted using
77 BioRad TC10 automated cell counter to determine the cell viability in the two control groups and
78 the AgNP exposed cells. Total cell count, total viable cell count, and cell viability percentage
79 were recorded.

80 *2.4 Oxidative stress measurement*

81 The H2DCFDA (2',7'-dichlorodihydrofluorescein diacetate) purchased from Invitrogen
82 (United States) was used for measuring oxidative stress level in HepG2 cells. Approximately
83 $2x10^4$ cells were seeded onto a 96-well plate and grown to ~70% confluence. Then treatment
84 with a citrate stabilizer control, a no treatment control, and with different doses (0.3 ppm to 5.0
85 ppm) of citrate stabilized AgNPs were conducted. The HepG2 cells were incubated at 37°C in 5%
86 CO_2 incubator upon treatment.

87 After 24 hours of treatment, the cells were further incubated with 200 μL of 100 mM
88 H2DCFDA (2',7'-dichlorodihydro fluorescein diacetate) dispersed in HBSS (Hank's Balanced
89 Salt Solution) for 30 min. The cells were then washed with PBS (Phosphate Buffer Saline) and
90 then transferred to complete growth media. The fluorescence intensity for each well was
91 obtained using an excitation at 485 nm and emission at 528 nm.

92 All fluorescence intensity measurements were normalized to the total protein present in
93 each well. After the fluorescence measurements, the cells were suspended in PBS and lysed by
94 sonication. The total amount of proteins in each well was then determined using BCA
95 (bicinchoninic acid) protein assay reagent.

96 *2.5 Protein extraction and proteomic analysis*

97 Approximately $4x10^6$ cells were seeded in a 135 mm dish and grown to approximately 70%
98 confluence and then dosed with 5.0 ppm citrate stabilized silver nanoparticles for 24h. The
99 undosed cells were used as control. After 24 hours of treatment, the cells were washed with ice
100 cold PBS and gently scraped from the dish. The cells were then centrifuged at 450 xg for 5 min
101 at 4^oC. Cell pellets were chemically lysed using Qproteome mammalian protein preparation kit
102 from Qiagen. The total protein in each sample was determined and normalized using BCA
103 protein assay reagent. The unfractionated protein samples were then sent to MSBioworks, LLC
104 for proteomic analysis.

105 During the proteomic analysis, these samples were mixed with LDS (lithium dodecyl
106 sulfate) buffer (sample loading buffer) and then loaded onto a 4-12% SDS-PAGE gel. Each gel
107 band was digested with trypsin and profiled using Protein-works Protein Profiling without
108 further fractionation. The gel digests were analyzed using nano LC/MS/MS with Waters
109 NanoAcquity HPLC system interfaced to a ThermoFisher Orbitrap Velos Pro using MSBioworks
110 protocols. Briefly, peptides were loaded on a trapping column and eluted from a 75 μm
111 analytical column at 350 nL/min with both columns packed with Jupiter Proteo Resin
112 (Phenomenex) employing a 1h gradient. The mass spectrometer was operated in data-dependent
113 mode, with MS performed in the Orbitrap at 60,000 FWHM resolution and MS/MS performed in
114 the LTQ. The fifteen most abundant ions were selected for MS/MS. The Mascot database

115 containing peptide mass fingerprints from Matrix Science Ltd. London was used in identifying
116 proteins characterized using MS/MS.

117 Spectral counting, a non-labeling relative protein quantification technique, was utilized in
118 this study. In spectral counting, the relative amount of protein in a sample is correlated with the
119 number of peptide spectra associated with that specific protein.

120 *2.6 Transmission Electron Microscope (TEM)*

121 TEM was used to investigate the morphological differences between the cells treated for 24
122 hours with 5.0 ppm AgNPs and the untreated cells. The cells were fixed using 4%
123 gluteraldehyde in 0.1 M PBS overnight and then post-fixed with 1% OsO_4 in 0.1M PBS for 1
124 hour. Cell pellets were dehydrated by suspending into 25%, 50%, 75%, 100% ethanol and 100%
125 propylene oxide consecutively for 15 min in each solution, 1:1, 2:1, and 0:1 EMBed 812 and
126 propylene oxide, for 2 hours and overnights, respectively. After dehydration, cell pellets were
127 embedded in beam capsules and dried with in the oven at 60°C for 4 hours, followed by
128 sectioning. Ultrathin sections (50-100 nm) were collected and images were obtained using a
129 Hitachi-7500 Transmission Electron Microscope (Hitachi, Ltd. Tokyo, Japan).

130

131 *2.7 Statistical analysis*

132 All the experiments were carried out independently at least 3 times. All numerical data
133 was presented as mean ± standard deviation. Whenever appropriate, the statistical significance
134 was determined by the Student's t-test at $p<0.05$.

135 **3. Results**

136 To study the potential toxicity mechanisms of AgNPs, HepG2 cells were exposed to
137 various doses of citrate stabilized AgNPs of 10nm. We examined the impact of these AgNPs as

138 a function of dose on the expression of different parameters of the HepG2 cell responses. The
139 results of these studies are reported below.

140 *3.1 Effects of AgNPs on HepG2 cell viability and proliferation*

141 The effects of increasing concentrations of AgNPs on the viability of HepG2 cells were
142 determined using a tryphan blue exclusion test. The exposure of the HepG2 cells to 10nm citrate
143 stabilized AgNPs resulted in observable cell death at doses > 1ppm after 24 hours of treatment.
144 The lethal dose (LD_{50}), in which only fifty percent (50%) of cells are viable, was observed at 3.0
145 ppm (Fig. 1).

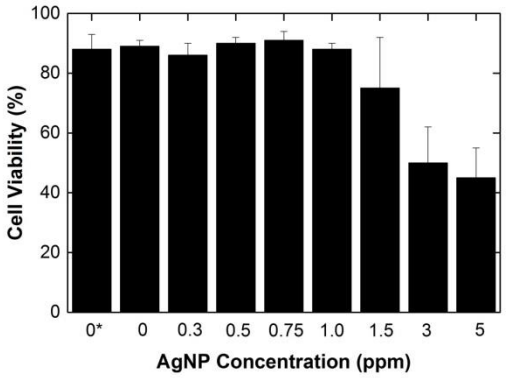

146

147 **Fig.1** Cell viability of HepG2 cells after 24h exposure to 10nm citrate-coated AgNPs. 0^* represents the
148 citrate stabilizer control.
149

150 Several investigators have reported cell viability studies on 24h AgNP treated HepG2 cells
151 using different nanoparticle sizes, stabilizers, manufacturers and assays. LD_{50} findings for the
152 same cells treated with 10nm AgNPs stabilized with water (Biocera Company, South Korea) is
153 2.5-3.0 ppm using MTT [3-(4,5-dimethylthiazol-2-yl)-2,5-diphenyltetrazolium bromide] and
154 XTT [2,3-bis-(2-methoxy-4-nitro-5-sulfophenyl)-2H-tetrazolium-5-carboxanilide] assay[66].
155 LD_{50} measured by Kawata, et al. was 2.5 ppm for 7-10nm AgNPs stabilized with
156 polyethylenimine (Kyoto Nanochemical Co., Ltd., Japan) using neutral red uptake assay [61]. IC_{50}

157 by Lin, et al. was > 30 ppm for 5nm AgNPs stabilized with water and SMA [poly(styrene-co-
158 maleic anhydride)-grafting poly(oxylkyalkylene)] (Gold Nanotech Industries) using MTT assay
159 [39]. LD_{50} by Eom, et al. was >20 ppm for 2nm AgNP stabilized by PVP (polyvinylpryrrolidone)
160 using MTT assay [67]. Our LD_{50} result of 3 ppm for 24h treatment with 10nm citrate-coated
161 AgNPs is in agreement with the results from these other investigators that used 10nm AgNPs
162 with different treatment time, stabilizers, and assays.

163 *3.2 Effects of AgNPs on oxidative stress in HepG2 cells*

164 Oxidative stress in Hep2G cells treated with different doses of AgNPs was determined
165 using H2DCFDA assay for reactive oxygen species (ROS). Exposure of HepG2 cells to
166 increasing doses of 10nm citrate stabilized AgNPs for 24h resulted in increasing ROS levels in
167 the cells (Fig. 2). Even at a low dose of 0.3 ppm, an increase in ROS level compared to the two
168 controls (citrate and 0ppm) is noticeable. The citrate stabilizer control was not significantly
169 different from the no treatment control. A maximum ROS level was reached at 3.0 ppm then
170 declined at 5.0 ppm, where a major portion of the population of cells were already dead. Pairing
171 this information with the cell viability response curve (Fig.1), where a noticeable decrease in cell
172 viability was observed at 1.5 ppm, indicates that HepG2 cells were able to withstand some higher
173 levels of ROS for short periods of time before cell death.

174

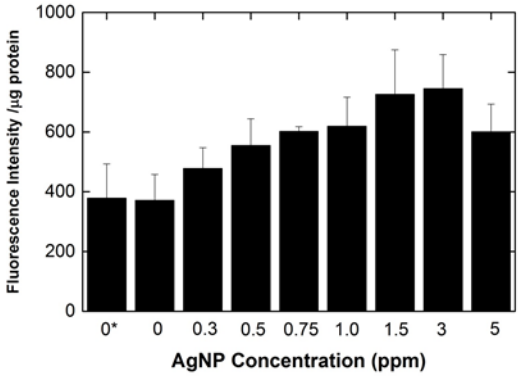

Fig. 2 Fluorescence intensity measured using H_2DCFDA for the oxidative stress level of HepG2 cells after 24h treatment using 10nm citrate stabilized AgNPs . 0^* represents the citrate control experiment.

Other investigators have studied the oxidative stress caused by AgNPs on cells and apoptosis induction. Nowrouwzi et al. found increasing NO levels, lipid peroxidation, and lower glutathione levels as cells were increasingly dosed with AgNPs[66]. Kim, et al. concluded that toxicity of AgNPs to HepG2 cells is mainly due to oxidative stress [68]. Hwang et al. found an increase of hydroxyl radicals that induce apoptotic cell death in the yeast Candida albicans [69]. Mukherjee et al. observed AgNP induced elevated levels of oxidative stress and depletion of glutathione in human dermal and cervical cancer cell lines [70]. Though different methods, cells, and AgNPs were used in the measurement of oxidative stress levels, all these studies consistently report that generation of ROS in the cell results from the exposure to AgNPs.

3.3 Effects of AgNPs on protein expression

To understand which proteins in HepG2 cells are potentially affected by exposure to silver nanoparticles, we performed protein extraction, identification, and quantification in order to find a clear trend. In the proteomic analysis, the protein samples were quantified and equal concentrations of protein were loaded onto a SDS gel and run to allow proteins to migrate a few centimeters. The proteins were then visualized with coommassie blue and the entire mobility

195 region excised and digested with trypsin and then prepared for LC mass spectrometry proteomic
196 analysis. Data obtained from the mass spectromic analysis was searched using a local copy of
197 Mascot with Enzyme trypsin, against the SwissProt human data base, including the
198 Carbamidomethyl (C) fixed modification, and variable modification of Oxidation (M),
199 Acetyl(Protein N-term), Pyro-Glu(N-term Q), and Deamidation (NQ) databases.

200 Using LC tandem mass spectrum and spectral counting approach we were able to identify a
201 total of 1218 proteins from both the treated and control HepG2 cells. The number of proteins
202 identified from the control was 1026; slightly more than the treated which was 987. In both
203 samples the false discovery rate (FDR) was 0.1%. The proteins affected by the treatment
204 included: membrane proteins, cytoplasmic, cytoskeletal, and some nuclear proteins. Among the
205 proteins observed, mitochondrial proteins such as 60 kDa heat shock protein were affected
206 significantly. Other affected proteins were fatty acid synthase, the tubulin beta chain, the histone
207 family proteins, spectrin family proteins, and other numerous proteins. Interestingly, some of the
208 proteins that showed large spectral count differences are involved in calcium dependent
209 movement of the cytoskeletal membrane, cell motility, protein structure control, ATPase cycle,
210 glycolysis, play role in RNA transcription and ribosome assembly, are involved in RNA
211 metabolism both in the nucleus and mitochondria, and others.

212 Culture of the control and treated cells began with equal numbers of cells and upon harvest
213 the number of cells prepared for proteomic analyses were comparable. To minimize the
214 difference in cell numbers, we used a proportional amount of protein extraction kits.
215 Furthermore, equal amounts of protein extract samples were loaded onto the SDS gel. These
216 steps were taken to minimize or control the differences caused by sample handling and
217 preparation and maintain the original expression differences. As a whole, the tubulin family

218 proteins were observed to be down expressed in the treated cells compared to the control cells
219 (Table 1). Tubulin family proteins are cytoskeletal proteins in the cytoplasm and are major
220 constituents of microtubules. As key components of the cytoskeleton, these long, filamentous,
221 tube-shaped polymer proteins are essential in all eukaryotic cells and are crucial in the
222 development and maintenance of cell shape, the transport of vesicles, mitochondria, and other
223 components throughout cells. They also play a critical role in cell signaling and in cell division
224 or mitosis. They are composed of alpha and beta tubulin dimers and their functionality is
225 determined by the expression and post translational modification of tubulin proteins [71].

226 **Table 1** Tubulin proteins' expression with and without the presence of AgNPs

Protein Accession Number	M.Wt (kDa)	Spectral Count 0 ppm	Spectral Count 5.0 ppm	Δ
sp|Q9BQE3|TBA1C_HUMAN	50	60	39	-21
sp|P07437|TBB5_HUMAN	50	77	53	-24
sp|Q13885|TBB2A_HUMAN	50	59	0	-59
sp|P68371|TBB2C_HUMAN	50	73	50	-23
sp|Q13509|TBB3_HUMAN	50	40	32	-8

227

228 The ribosomal protein family (40 S ribosomal proteins) was also down expressed after the
229 treatment of AgNPs. These proteins are Proteins of the ribosome, large ribonucleo-protein
230 particles where the translation of messenger RNA (mRNA) into protein occurs. They are both
231 free in the cytoplasm and attached to the membranes of eukaryotic and prokaryotic cells. A total
232 of 26 proteins were identified and quantified in this family and all were found to be under

expressed in the treated sample compared to the control. Depending on their post translational modification they have different functionality and importance.

In contrast to the tubulin and ribosomal proteins, four heat shock proteins were found to be overly expressed in the treated sample relative to the control (Table 2).

Table 2 Most affected heat shock proteins' expression in the presence of AgNPs

Protein Accession Number	M.Wt (kDa)	Spectral count 0 ppm	Spectral count 5.0 ppm	Δ
sp|P08107|HSP71_HUMAN	70	28	51	+23
sp|P11142|HSP7C_HUMAN	71	30	41	+11
sp|P07900|HS90A_HUMAN	85	62	79	+17
sp|P08238|HS90B_HUMAN	83	90	98	+8

3.4 Agglomeration of AgNPs in HepG2 cells

In order to understand the toxicity mechanisms of AgNPs to the HepG2 cells, we used the images obtained by Transmission Electron Microscope (TEM) to locate the AgNPs in HepG2 cells. Three representative TEM images are shown in Fig. 3, which correspond to a control (Fig. 3A) and a 5.0 ppm dosed HepG2 cell (Figs. 3B and3C).

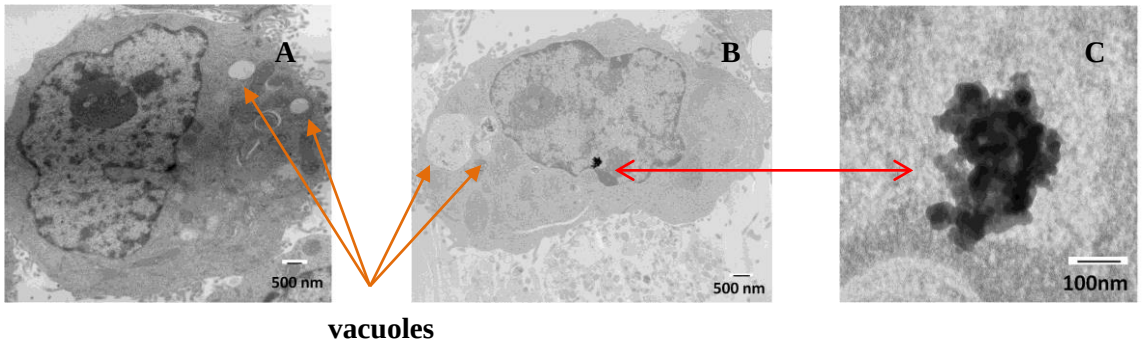

Fig. 3 TEM images of control (A) and 5.0 ppm AgNP dosed HepG2 cell (B & C).

Agglomerated citrate stabilized AgNPs were found to penetrate the treated HepG2 cells. Several recent studies have also shown that AgNPs with the size of 10 nm can penetrate inside of the cells [72-73]. Furthermore, Fig. 3 B and C show an agglomeration of AgNPs near or inside the nucleus with a size of about 300 nm. The treated cells were observed to shrink in size, a diameter of ~7 nm in comparison to that of 10-13 nm of the control cells. Moreover, an expansion of the vacuole containing a large amount of lysosomes which are responsible for intracellular processing of waste was also noticeable in the treated cells. This change in cell morphology in the treated cells is an indication that the dose used (5 ppm) is toxic to the cells.

4. Discussion and conclusion

The present study showed the exposure of HepG2 cells to 10nm citrate-coated AgNPs is toxic at a dose of above 1ppm based on the ROS measurements. Furthermore, the LD_{50} was observed to be 3 ppm when these AgNPs were exposed to HepG2 cells for 24 hours. The widely accepted mechanism of AgNP toxicity is the release of Ag cations that dissolve from the passivated AgNPs. This toxicity pathway is likely as the results in the study by Gliga, et al.[74] demonstrated that 10nm AgNPs release more Ag cations than the AgNPs of larger sizes. However, this pathway alone cannot explain the toxicity of 10nm AgNPs coated with citrate and PVP, which release Ag cations by different rates. While the mode of toxicity is independent of coating materials, the citrate-coated AgNPs release more Ag cations than the PVP-coated do in a given time period. Furthermore, the release of Ag cations by 10nm AgNPs coated with PVP in HepG2 cells is about 10% of maximum [75]. This suggests that other pathways are also responsible to the toxicity of AgNPs. As ligands affect properties and functions of nanoparticles[76-78], further studies of AgNP with different coating will be interesting.

The TEM images in this work illustrated the aggregation of AgNPs inside the HepG2 cells. This leads us to hypothesize that osmotic pressure generated by the aggregation of AgNPs inside the HepG2 cells may induce toxicity. The change in osmotic potential resulted in the loss of water inside the HepG2 cells that leads to a smaller size of HepG2 cells. Upon a closer examination of the TEM images of HepG2 cells, we indeed found smaller sizes of the treated HepG2 cells and thus confirmed this hypothesis. A previous study by Cheng, et al. demonstrated that an aggregation of PVP-coated AgNPs under sunlight can reduce toxicity[49], which further supports our hypothesis. As such, we expect the reduction of the toxicity of AgNPs under the proposed toxicity mechanism can be achieved by preventing the aggregation of small nanoparticles or utilizing the nanoparticles in a size range that is not likely to aggregate.

This work also showed that the exposure to 10nm citrate-coated AgNPs resulted in oxidative stress even at a lower dose of 0.3 ppm. Normal protein expression of HepG2 cells were also affected by the exposure of these AgNPs. Expression of heat shock protein, fatty acid synthase, and histone and spectrin proteins were affected upon exposure of HepG2 cells to 5 ppm of 10nm citrate-coated AgNPs. A similar observation was reported in other studies where AgNPs can induce dose dependent oxidative stress and up regulation of heat shock proteins upon exposure to AgNPs[2, 79].

In conclusion, our results show that the toxic dosage of 10nm citrate-coated AgNPs to HepG2 cells after 24h exposure starts at >1ppm and LD_{50} is 3ppm. Evidence of the toxicity of AgNPs to HepG2 cells was supported by the oxidative stress levels, cell morphology changes, and protein expression changes affected in HepG2 cells. Oxidative stress levels in the cells were observed to increase in a dose-dependent way to AgNPs and further that high doses led to cell death. AgNPs were able to penetrate the cells and aggregate. Treated HepG2 cells were smaller

and exhibited larger and more numerous vacuoles containing increased amounts of lysosomes shown in the TEM images. Important proteins affected upon the exposure of AgNPs to HepG2 cells were a family of heat shock proteins, tubulin proteins, histones, and spectrins. Osmotic pressure generated by the aggregation of AgNPs inside HepG2 cells is proposed to be an important toxicity mechanism of 10nm citrate-coated AgNPs.

Conflicts of interest statement

The authors declare that there are no conflicts of interest.

Acknowledgements

We thank Sara Ladley for her assistance on HepG2 cell culture. Part of the work was supported by a National Science Foundation grant (CBET-0709113).

References

1. Cho, J. H.; Kulkarni, A.; Kim, H.; Yoon, J. U.; Sung, J. H.; Yu, I. J.; Kim, T., Numerical Study on Spatial Distribution of Silver Nanoparticles inside Whole-Body Type Inhilation Toxicity Chamber. *J. Mech. Sci. Tech.* **2010**, *24*, 2215-2220.
2. Ahmed, M.; Posgai, R.; Gorey, T. J.; Nielsen, M.; Hussain, S. M.; Rowe, J. J., Silver Nanoparticles Induced Heat Shock Protein 70, Oxidative Stress and Apoptosis in Drosophilia Melanogaster. *Toxicol. Appl. Pharma.* **2009**, *242*, 263-269.
3. Shimoga, G.; Palem, R. R.; Lee, S.-H.; Kim, S.-Y., Catalytic Degradability of P-Nitrophenol Using Ecofriendly Silver Nanoparticles. *Metals* **2020**, *10*, 1661.
4. Gherasim, O.; Puiu, R. A.; Bîrcă, A. C.; Burdușel, A.-C.; Grumezescu, A. M., An Updated Review on Silver Nanoparticles in Biomedicine. *Nanomater.* **2020**, *10*, 2318.
5. Derakhshan, M. A.; Amani, A.; Faridi-Majidi, R., State-of-the-Art of Nanodiagnostics and Nanotherapeutics against Sars-Cov-2. *ACS Appl. Mater. Interfaces* **2021**, *13*, 14816-14843.
6. Miranda, R. R.; Sampaio, I.; Zucolotto, V., Exploring Silver Nanoparticles for Cancer Therapy and Diagnosis. *Colloids Surf. B: Biointerfaces* **2022**, *210*, 112254.
7. Akintelu, S. A.; Olugbeko, S. C.; Folorunso, A. S.; Oyebamiji, A. K.; Folorunso, F. A., Potentials of Phytosynthesized Silver Nanoparticles in Biomedical Fields: A Review. *Int. Nano Lett.* **2021**, *11*, 273-293.

8. Tortella, G. R.; Pieretti, J. C.; Rubilar, O.; Fernandez-Baldo, M.; Benavides-Mendoza, A.; Dieza, M. C.; Seabra, A. B., Silver, Copper and Copper Oxide Nanoparticles in the Fight against Human Viruses: Progress and Perspectives. *Critical Rev. Biotechnol.* **2022**, *42*, 431-449.
9. Yang, X.; Jia, M.; Li, Z.; Ma, Z.; Lv, J.; Jia, D.; He, D.; Zeng, R.; Luo, G.; Yu, Y., In-Situ Synthesis Silver Nanoparticles in Chitosan/Bletilla Striata Polysaccharide Composited Microneedles for Infected and Susceptible Wound Healing. *Int. J. Biolog. Macromol.* **2022**, *215*, 550-559.
10. Shi, Y.; Lyu, Z.; Zhao, M.; Chen, R.; Nguyen, Q. N.; Xia, Y., Noble-Metal Nanocrystals with Controlled Shapes for Catalytic and Electrocatalytic Applications. *Chem. Rev.* **2021**, *121*, 649-735.
11. Zhou, S.; Li, J.; Gilroy, K. D.; Tao, J.; Zhu, C.; Yang, X.; Sun, X.; Xia, Y., Facile Synthesis of Silver Nanocubes with Sharp Corners and Edges in an Aqueous Solution. *ACS Nano* **2016**, *10*, 9861-9870.
12. Lu, J.; Aydin, C.; Browning, N. D.; Wang, L.; Gates, B. C., Sinter-Resistant Catalysts: Supported Iridium Nanoclusters with Intrinsically Limited Sizes. *Catal. Lett.* **2012**, *142*, 1445-1451.
13. Xiao, L.; Wang, L., Structures of Platinum Clusters: Planar or Spherical? *J. Phys. Chem. A* **2004**, *108*, 8605-8614.
14. Pawluk, T.; Hirata, Y.; Wang, L., Studies of Iridium Nanoparticles Using Density Functional Theory Calculations. *J. Phys. Chem. B* **2005**, *109*, 20817-20823.
15. Wang, L.; Ore, R. M.; Jayamaha, P. K.; Wu, Z.-P.; Zhong, C.-J., Density Functional Theory Based Computational Investigations on the Stability of Highly Active Trimetallic Ptpdcu Nanoalloys for Electrochemical Oxygen Reduction. *Faraday Discuss.* **2022**, DOI: 10.1039/d2fd00101b.
16. Wang, L.; Williams, J. I.; Lin, T.; Zhong, C. J., Spontaneous Reduction of O_2 on Ptvfe Nanocatalysts. *Catal. Today* **2011**, *165*, 150-159.
17. Wu, R.; Wang, L., Insight and Activation Energy Surface of the Dehydrogenation of C_2h_xo Species in Ethanol Oxidation Reaction on Ir(100). *ChemPhysChem* **2022**, e202200132.
18. Wu, R.; Wiegand, K. R.; Ge, L.; Wang, L., Role of Oxygen Species toward the C-C Bond Cleavage in Steam Reforming of C_{2+} Alkanes: Dft Studies of Ethane on Ir(100). *J. Phys. Chem. C* **2021**, *125*, 14275-14286.
19. Wu, R.; Sun, K.; Chen, Y.; Zhang, M.; Wang, L., Ethanol Dimerization to Ethyl Acetate and Hydrogen on the Multifaceted Copper Catalysts. *Surf. Sci.* **2021**, *703*, 121742.
20. Sun, K.; Zhang, M.; Wang, L., Effects of Catalyst Surface and Hydrogen Bond on Ethanol Dehydrogenation to Ethoxy on Cu Catalysts. *Chem. Phys. Lett.* **2013**, *585*, 89-94.
21. Miao, B.; Wu, Z.; Zhang, M.; Chen, Y.; Wang, L., Role of Ni in Bimetallic Pdni Catalysts for Ethanol Oxidation Reaction. *J. Phys. Chem. C* **2018**, *122*, 22448-22459.
22. Wu, Z.-P.; Miao, B.; Hopkins, E.; Park, K.; Chen, Y.; Jiang, H.; Zhang, M.; Zhong, C.-J.; Wang, L., Poisonous Species in Complete Ethanol Oxidation Reaction on Palladium Catalysts. *J. Phys. Chem. C* **2019**, *123*, 20853-20868.
23. Wu, R.; Wiegand, K. R.; Wang, L., Impact of the Degree of Dehydrogenation in Ethanol C-C Bond Cleavage on Ir(100). *J. Chem. Phys.* **2021**, *154*, 054705.
24. Miao, B.; Wu, Z.; Xu, H.; Zhang, M.; Chen, Y.; Wang, L., Ir Catalysts: Preventing Ch_3cooh Formation in Ethanol Oxidation. *Chem. Phys. Lett.* **2017**, *688*, 92-97.

25. Wu, R.; Wang, L., A Density Functional Theory Study on the Mechanism of Complete Ethanol Oxidation on Ir(100): Surface Diffusion-Controlled C-C Bond Cleavage *J. Phys. Chem. C* **2020**, *124*, 26953-26964.
26. Wu, Z.; Zhang, M.; Jiang, H.; Zhong, C.-J.; Chen, Y.; Wang, L., Competitive C–C and C–H Bond Scission in the Ethanol Oxidation Reaction on Cu(100) and the Effect of an Alkaline Environment. *Phys. Chem. Chem. Phys.* **2017**, *19*, 15444-15453.
27. Miao, B.; Wu, Z.-P.; Xu, H.; Zhang, M.; Chen, Y.; Wang, L., Dft Studies on the Key Competing Reaction Steps Towards Complete Ethanol Oxidation on Transition Metal Catalysts. *Comput. Mater. Sci.* **2019**, *156*, 175-186.
28. Wu, R.; Wang, L., Alloying Effect Via Comparative Studies of Ethanol Dehydrogenation on Cu(111), Cu_3Pd(111), and Cu_3Pt(111). *Chem. Phys. Lett.* **2017**, *678*, 196-202.
29. Gogoi, S. K.; Gopinath, P.; Paul, A.; Ramesh, A.; Ghosh, S. S.; Chattopadhyay, A., Green Flourescent Protein-Expressing Escherichia Coli as a Model System for Investigating the Antimicrobial Activities of Silver Nanoparticles. *Langmuir* **2006**, *22*, 9322-9328.
30. Singh, M.; Singh, S.; Prasad, S.; Gambhir, I. S., Nanotechnology in Medicine and Antibacterial Effect of Silver Nanoparticles. *Dig. J. Nanomater. Biostructures* **2008**, *3*, 115-122.
31. Sondi, I.; Salopek-Sondi, B., Silver Nanoparticles as Antimicrobial Agent: A Case Study on E. Coli as a Model for Gram-Negative Bacteria. *J. Colloid Interface Sci.* **2004**, *275*, 177-182.
32. Ugyun, M.; Kahveci, M. U.; Odaci, D.; Tumur, S.; Yagci, Y., Antibacterial Acrylamide Hydrogels Containing Silver Nanoparticles by Simultaneous Photoinduced Free Radical Polymerization and Electron Transfer Process. *Macromol. Chem. Phys.* **2009**, *210*, 1867-1875.
33. Kim, J. S.; Kuk, E.; Yu, K. N.; Kim, J. H.; Park, S. J.; Lee, H. J.; Kim, S. H.; Park, Y. K.; Park, Y. H.; Hwang, C. Y., Antibacterial Effects of Silvernanoparticles. *Nanomedicine* **2007**, 95-101.
34. Lok, C. N.; Ho, C. M.; Chen, R.; He, Q. Y.; Yu, W. Y.; Sun, H.; Tam, P. K.; Chiu, J. F.; Chen, C. M., Proteomic Analysis of the Mode of Antibacterial Action of Silver Nanoparticles. *J. Proteome. Res.* **2006**, *5*, 916-924.
35. Travan, A.; Pelillo, C.; Donati, I.; Marsich, E.; Benincasa, M.; Scarpa, T.; Semeraro, S.; Turco, G.; Gennaro, R.; Paoletti, S., Noncytotoxic Silver Nanoparticles-Polysaccharide Nanocomposite with Antimicrobial Activity. *Biomacromolecules* **2009**, *10*, 1429-1435.
36. El Badawy, A. M.; Silva, R. V.; Morris, B.; Scheckel, K. G.; Suidan, M. T.; Tolaymat, T. M., Surface Charge-Dependent Toxicity of Silver Nanoparticles. *Environ. Sci. Technol.* **2011**, *45*, 283-287.
37. Mo, L.; Liu, D.; Li, W.; Li, L.; Wang, L.; Zhou, X., Effects of Dodecylamine and Dodecanethiol on the Conductive Properties of Nano-Ag Films. *Appl. Surf. Sci.* **2011**, *257*, 5746-5753.
38. Merill, J. C.; Morton, J. J. P.; Solleau, S. D., *Metals*; Taylor & Francis Group: Boca Raton, 2008.
39. Lin, J.; Lin, W.; Dong, R.; Hsu, S., The Cellular Responses and Antibacterial Activities of Silver Nanoparticles Stabilized by Different Polymers. *Nanotechnol.* **2012**, *23*, 1-12.
40. Nanowerk Groups File Legal Action for Epa to Stop Sale of 200+ Nanosilver Products. http://www.nanowerk.com/news/newsid=5559.php (accessed 2022 November 23).
41. Johnston, H. J.; Hutchison, G.; Christensen, F. M.; Peters, S.; Hankin, S.; Stone, V., A Review of the in Vivo- and in Vitro Toxicity of Silver and Gold Particulates: Particle

413 Attributes and Biological Mechanismns Reponsible for the Observed Toxicity. *Crit. Rev.*
414 *Toxicol.* **2010**, *40*, 328-346.
415 42. Lankoff, A.; Sandberg, W. J.; Wegierek-Ciuk, A.; Lisowska, H.; Sartowska, B.; Schwarze, P.
416 E.; Meczynska-Wielgosz, S.; Wojewodzka, M., The Effect of Agglomeration State of Silver
417 and Titanium Oxide Nanoparticles on Cellular Response of of HepG2, A549 and Thp-1 Cells.
418 *Toxicol. Lett.* **2012**, *208*, 197-213.
419 43. Stone, V.; Johnston, H.; Clift, M. J., Air Pollution, Ultrafine and Nanoparticle Toxicology:
420 Cellular and Molecular Interactions. *IEEE Trans. Nanobiosci.* **2007**, *6*, 331-340.
421 44. Piao, M. J.; Kang, K. A.; Lee, I. K.; Kim, H. S.; Kim, S.; Choi, J. Y.; Choi, J.; Hyun, J. W.,
422 Silver Nanoparticles Induce Oxidative Cell Damage in Human Liver Cells through Inhibition
423 of Reduced Glutathione and Induction of Mitochondria-Involved Apoptosis *Toxicol. Lett.*
424 **2011**, *201*.
425 45. Garza-Ocanas, L.; Ferrer, D. A.; Burt, J.; Diaz-Torres, L. A.; Cabrera, M. R.; Rodrı´guez, V.
426 T.; Rangel, R. L.; Romanovicze, D.; Jose-Yacaman, M., Biodistribution and Long Term Fate
427 of Silver Nanoparticles Functionalized with Bovine Serum Albumin in Rats. *Metallomics*
428 **2010**, *2*, 204-210.
429 46. Ashani, P. V.; Low Kah Mun, G.; Hande, M. P., Cytotoxicity and Genotoxicity of Silver
430 Nanoparticles in Human Cells *ACS Nano* **2009**, *3*, 279-290.
431 47. Kramer, J.; Bell, R.; Smith, S.; Gorsuch, J., Silver Nanoparticle Toxicity and Biocides: Need
432 for Chemical Speciation. *Integr. Environ. Asses. Manag.* **2009**, *4*, 720-722.
433 48. Arora, S., Jain, J., Rajwade, J. M., and Paknikar, K. M., , Cellular Responses Induced by
434 Silver Nanoparticles: In Vitro Studies. *Toxicol. Lett.* **2008**, *179*, 93-100.
435 49. Cheng, Y.; Yin, L.; Lin, S.; Wiesner, M.; Berhardt, E.; Liu, J., Toxicity Reduction of
436 Polymer-Stablized Silver Nanoparticles by Sunlight. *J. Phys. Chem. C* **2011**, *115*, 4425-4432.
437 50. Jaswal, T.; Gupta, J., A Review on the Toxicity of Silver Nanoparticles on Human Health.
438 *Mater. Today: Proceedings* **2021**, https://doi.org/10.1016/j.matpr.2021.04.266.
439 51. Badawy, A. M. E.; Silva, R. G.; Morris, B.; Scheckel, K. G.; Suidan, M. T.; Tolaymat, T. M.,
440 Surface Charge-Dependent Toxicity of Silver Nanoparticles. *Environ. Sci. Technol.* **2011**, *45*,
441 283-287.
442 52. Stensberg, M. C.; Wei, Q.; McLamore, E. S.; Porterfield, D. M.; Wei, A.; lveda, M. S. S.,
443 Toxicological Studies on Silver Nanoparticles: Challenges and Opportunities in Assessment,
444 Monitoring and Imaging. *Nanomedicine (Lond)* **2011**, *6*, 879-898.
445 53. Ferdous, Z.; Nemmar, A., Health Impact of Silver Nanoparticles: A Review of the
446 Biodistribution and Toxicity Following Various Routes of Exposure. *Int. J. Mol. Sci.* **2020**,
447 *21*, 2375.
448 54. Bruna, T.; Maldonado-Bravo, F.; Jara, P.; Caro, N., Silver Nanoparticles and Their
449 Antibacterial Applications. *Int. J. Mol. Sci.* **2021**, *22*, 7202.
450 55. Báez, D. F.; Gallardo-Toledo, E.; Oyarzún, M. P.; Araya, E.; Kogan, M. J., The Influence of
451 Size and Chemical Composition of Silver and Gold Nanoparticles on in Vivo Toxicity with
452 Potential Applications to Central Nervous System Diseases. *Int. J. Nanomedicine* **2021**, *16*,
453 2187-2201.
454 56. Ghobashy, M. M., et al., An Overview of Methods for Production and Detection of Silver
455 Nanoparticles, with Emphasis on Their Fate and Toxicological Effects on Human, Soil, and
456 Aquatic Environment. *Nanotechnol. Rev.* **2021**, *10*, 954-977.
457 57. Toro, R. G., et al., Evaluation of Long–Lasting Antibacterial Properties and Cytotoxic
458 Behavior of Functionalized Silver-Nanocellulose Composite. *Mater.* **2021**, *14*, 4198.

58. Lui, W.; Wu, Y.; Wang, C.; Ling, H.; Wang, T.; Liao, C. Y.; Cui, L.; Zhou, Q. F.; Yan, B.; Jiang, G. B., Impact of Silver Nanoparticles on Human Cells: Effect of Particle Size. *Nanotoxicol.* **2010**, *4*, 319-330.
59. Lu, W.; Senapati, D.; Wang, S.; Tovmachenko, O.; K., S. A.; Yu, H.; Ray, P. C., Effect of Surface Coating on the Toxicity of Silver Nanomaterials on Human Skin Keratinocytes. *Chem. Phys. Lett.* **2010**, *487*, 92-96.
60. Ramzan, U., et al., New Insights for Exploring the Risks of Bioaccumulation, Molecular Mechanisms, and Cellular Toxicities of Agnps in Aquatic Ecosystem. *Water* **2022**, *14*, 2192.
61. Kawata, K.; Osawa, M.; Okabe, S., In Vitro Toxicity of Silver Nanoparticles at Noncytotoxic Doses to Hepg2 Human Hepatoma Cells. *Environ. Sci. Technol.* **2009**, *43*, 6046-6051.
62. Kittler, S.; Greulich, C.; Diendorf, J.; Koller, M.; Epple, M., Toxicity of Silver Nanoparticles Increases During Storage Because If Slow Dissolution under Release of Silver Ions. *Chem. Mater.* **2010**, *22*, 4548-4554.
63. Panyala, N. R.; Pena-Mendez, E. M.; Havel, J., Review: Silver or Silver Nanoparticles: A Hazardous Threat to the Environment and Human Health? *J. Appl. Biomed.* **2008**, *6*, 117-129.
64. Bouwmeester, H.; Poortman, J.; Peters, R.; Wijima, E.; Kramer., E.; Makama, S.; Puspitaninganindita, K.; Marvin, H. J. P.; Peingjnenburg, A. A. C. M.; Hendriksen, J. M., Characterization of Translocation of Silver Nanoparticles and Effects on Whole Genome Gene Expression Using in Vitro Intestinal Epithelium Coculture Model *ACS Nano* **2011**, *5*, 4091-4103.
65. Beer, C.; Foldbjerg, R.; Hayashi, Y.; Sutherland, D. S.; Autrup, H., Toxicity of Silver Nanoparticles - Nanoparticle or Silver Ion. *Toxicol. Lett.* **2012**, *208*, 286-292.
66. Nowrouzi, A., Meghrazi, K., Golmohammadi, T., Golestani, A., Ahmadian, S., Shafiezadeh, M., Shajary, Z., Khaghani, S., and Amiri, A. N., Cytotoxicity of Subtoxic Agnp in Human Hepatoma Cell Line (Hepg2) after Long-Term Exposure. *Iranian Biomedical J.* **2010**, *14*, 23-32.
67. Eom, H.; Choi., J., P38 Mapk Activation, DNA Damage, Cell Cycle Arrest and Apoptosis as Mechanism of Toxicity of Silver Nanoparticles in Jurkat T. Cells. *Environ. Sci. Technol.* **2010**, *44*, 8337-8342.
68. Kim, S.; Choi, J. E.; Choi, J.; Cheng, K. H.; Park, K.; Yi, J.; Ryu, D. Y., Oxidative Stress-Dependent Toxicity of Silver Nanoparticles in Human Hepatoma Cells. *Toxicol. In Vitro* **2009**, *23*, 1076-1084.
69. Hwang, I.; Lee, J.; Hwang, J. J.; Kim, K.; Lee, D. G., Silver Nanoparticles Induced Apoptotic Cell Death in Candida Albicans through Increase of Hydroxy Radicals. *FEBS J.* **2012**, *279*, 1327-1338.
70. Mukherjee, S. G.; O'claonadh, N.; Casey, A.; Chambers, D., Comparative in Vitro Cytotoxicity Study of Silver Nanoparticle on Two Mammalian Cell Lines. *Toxicol. In Vitro* **2012**, *26*, 238-251.
71. Jordan, M. A.; Wilson, L., Microtubules as a Target for Anticancer Drugs. *Nature Rev. Cancer* **2004**, *4*, 253-265.
72. Ivask, A., et al., Size-Dependent Toxicity of Silver Nanoparticles to Bacteria, Yeast, Algae, Crustaceans and Mammalian Cells *in Vitro*. *PLoS ONE* **2014**, *9*, e102108.
73. Miethling-Graffa, R.; Rumpkera, R.; Richtera, M.; Verano-Bragab, T.; Kjeldsenb, F.; Brewerc, J.; Hoylandd, J.; Rubahnd, H.-G.; Erdmanna, H., Exposure to Silver Nanoparticles Induces Size- and Dose-Dependent Oxidative Stress and Cytotoxicity in Human Colon Carcinoma Cells. *Toxicol. In Vitro* **2014**, *28*, 1280-1289.

74. Gliga, A. R.; Skoglund, S.; Wallinder, I. O.; Fadeel, B.; Karlsson, H. L., Size-Dependent Cytotoxicity of Silver Nanoparticles in Human Lung Cells: The Role of Cellular Uptake, Agglomeration and Ag Release. *Particle Fibre Toxicol.* **2014**, *11*, 11.
75. Yu, S.-j.; Chao, J.-b.; Sun, J.; Yin, Y.-g.; Liu, J.-f.; Jiang, G.-b., Quantification of the Uptake of Silver Nanoparticles and Ions to Hepg2 Cells. *Environ. Sci. Technol.* **2013**, *47*, 3268-3274.
76. Yang, T. H.; Shi, Y.; Janssen, A.; Xia, Y., Surface Capping Agents and Their Roles in Shape - Controlled Synthesis of Colloidal Metal Nanocrystals. *Angew. Chem. Int. Ed.* **2020**, *59*, 15378-15401.
77. Yuan, B.; Zhuang, J.; Kirmess, K. M.; Bridgmohan, C. N.; Whalley, A. C.; Wang, L.; Plunkett, K. N., Pentaleno[1,2-A:4,5′]Diacenaphthylenes: Uniquely Stabilized Pentalene Derivatives. *J. Org. Chem.* **2016**, *81*, 8312-8318.
78. Spivey, K.; Williams, J. I.; Wang, L., Structures of Undecagold Clusters: Ligand Effect. *Chem. Phys. Lett.* **2006**, *432*, 163-166.
79. Xin, L.; Wang, J.; Wu, Y.; Guo, S.; Tong, J., Increased Oxidative Stress and Activated Heat Shock Proteins in Human Cell Lines by Silver Nanoparticles. *Hum. Exp. Toxicol.* **2015**, *34*, 315-323.